Finding Limiting Flows of Batch Extractive Distillation with Interval Arithmetic

Erika R. Frits, Zoltán Lelkes, Zsolt Fonyó, and Endre Rév
Dept. of Chemical Engineering, Budapest University of Technology and Economics, H-1521 Budapest, Hungary

Mihály Cs. Markót
Computer and Automation Research Institute, Hungarian Academy of Sciences, H-1518 Budapest, Hungary

Tibor Csendes
Institute of Informatics, University of Szeged, H-6701 Szeged, Hungary

DOI 10.1002/aic.10917
Published online June 16, 2006 in Wiley InterScience (www.interscience.wiley.com).

A feasibility study on batch extractive distillation is based on analyzing profile maps. The existence and location of singular points and separatrices in these maps depend on process parameters. The limiting flows of the process are related to those parameter values where the map changes shape. Graphical tools can be used to roughly estimate these values. If a singularity is not found using graphical methods, one cannot guarantee that a singularity does not exist. Reliable computation of all zeroes of a nonlinear multidimensional function can be used to determine these points. This can be accomplished using interval arithmetic. An interval arithmetic–based branch-and-bound optimizer is applied to find the singular points and bifurcations. All the singular points of the maps at specified process parameters are found in this way. Limiting flows are determined with the same methodology by finding the bifurcation points and the corresponding parameter values. © 2006 American Institute of Chemical Engineers *AIChE J,* 52: 3100–3108, 2006
Keywords: interval arithmetic, extractive distillation, feasibility, bifurcation, profile map

Introduction

Batch extractive distillation (BED) is a unit operation applicable to separate close boiling and azeotrope forming mixtures. The separation is performed using a third liquid component called an *entrainer*. The entrainer can be either the least volatile, the most volatile, or even the intermediately volatile component in the ternary system.[1] This article deals with separating minimum boiling azeotropes applying a heavy entrainer. Figure 1 illustrates the model arrangement.

The process itself is performed as follows.[2] The charge is first put in the still vessel, and the column is heated up with total reflux. As a result, the top composition approaches the azeotrope. The entrainer is continuously fed to the column in the next step, although the distillate is not yet produced. The bottom composition moves toward the entrainer vertex because most of the entrainer accumulates in the still vessel. Once the top composition reaches its specified value, production is started with a well-designed reflux ratio ($R = L/D$) and feed ratio (F/V). Of the acetone (A)–methanol (B)–water (E) system, almost pure component A is produced in this step. As a result of distillate removal, the still composition turns toward the BE edge of the composition triangle. During this step, the distillate composition remains nearly constant.

Feeding of the entrainer is stopped when distillate purity starts to decrease. The receiver is changed and an off-cut is

E. R. Frits, Z. Fonyó, and E. Rév are also affiliated with the joint Hungarian Academy of Sciences–Budapest University of Technology and Economics (HAS–BUTE) Research Group of Technical Chemistry, H-1521 Budapest, Hungary.
Correspondence concerning this article should be addressed to E. R. Frits at efrits@mail.bme.hu and E. Rév at ufo@mail.bme.hu.

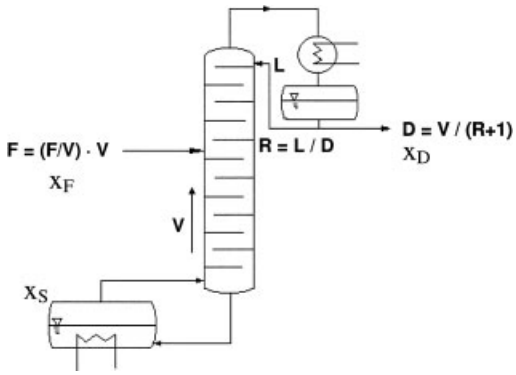

Figure 1. BED in a rectifier.

removed. As a result, the still becomes free of component A. Component B is then distilled out with conventional batch distillation and the entrainer remains in the still.

Feasibility of the process depends on R and F/V. Simulation or experimental trials with randomly selected parameter values typically lead to the conclusion that the process is infeasible, although it is really feasible with appropriately selected process parameters. This is why limiting values of these parameters are important to explore.

The appropriate process parameters can be roughly estimated by analyzing profile maps. The location of the singular points—and the parameter values where some singular points appear or disappear—play a key role in assessing feasibility. Appearance and disappearance of singular points are called *bifurcations*. The singular points, especially the saddle points, cannot always be determined with satisfactory precision. Some details of the map are missed because unstable nodes are not determined.

Bifurcation cannot always be recognized because the computed maps are not sufficiently detailed. More precise determination of their loci involves extensive computation with a finer mesh in the studied composition and parameter domain. Existence of a singular point cannot be excluded merely on the basis of not finding it with a given mesh over the studied domain. In contrast to this lack of information, *interval arithmetic* has the potential of excluding the existence of some solutions and of finding the bifurcation points according to their mathematical criteria.

Graphical Feasibility Methodology

The feasible domain of R and F/V, as well as the feasible region of still compositions, can be estimated by analyzing the profile maps.[2-4]

Such a map includes a curve approximating the rectifying profile started from a specified distillate composition $\mathbf{x}_D$. This curve can be computed by numerically solving the differential Eq. 1 with initial value $\mathbf{x}_D$:

$$\frac{d\mathbf{x}}{dh} = \frac{V}{L}[\mathbf{y}(\mathbf{x}) - \mathbf{y}^*(\mathbf{x})] \tag{1}$$

where h is dimensionless height, L is liquid flow rate, $\mathbf{y}^*(\mathbf{x})$ is equilibrium vapor composition, and $\mathbf{y}(\mathbf{x})$ is actual vapor composition according to the column's component balance (operating line) above the feed:

$$\mathbf{y} = \frac{R}{R+1}\mathbf{x} + \frac{1}{R+1}\mathbf{x}_D \tag{2}$$

The map also includes a sequence of curves approximating the extractive profiles started from potential still compositions. Such a curve can be computed by numerically solving the same differential Eq. 1 in the reverse direction with the potential still composition $\mathbf{x}_S$ as initial value and with the actual vapor composition determined according to the balance (operating line) below the feed:

$$\mathbf{y} = \left(\frac{R}{R+1} + \frac{F}{V}\right)\mathbf{x} + \frac{1}{R+1}\mathbf{x}_D - \frac{F}{V}\mathbf{x}_F \tag{3}$$

Any still composition $\mathbf{x}_S$ is called *feasible* if the computed extractive profile meets the rectifying profile.

Feasibility studies are usually started with computing and visualizing the profile maps at total reflux, with several different feed ratios. When F/V approaches zero in Eq. 3 at total reflux ($R = \infty$), a *limit map* is formed. This limit map is equivalent to the reversed-direction residue curves map. All these limit curves start from the neighborhood of vertex E, pass either vertex B or vertex A, and approach the azeotropic composition. Vertex E is an unstable node (UN); the azeotrope is a stable node (SN); vertices A and B are saddle points S_1 and S_2, respectively.

As the feed ratio (F/V) changes, saddle points S_1 and S_2 move along the binary AE and BE edges, respectively. The unstable node UN remains in place, but SN moves in the interior of the triangle. Stable node SN moves along the isovolatility curve and reaches the BE edge at some particular feed ratio. This is demonstrated numerically by Safrit el al.[5] and proven theoretically by Lelkes et al.[2]

The extractive profile computed from the still composition should meet the rectifying profile if it is a part of a feasible column profile. To obtain such an intersection between the two profiles, stable node SN should move down very near to the AE edge. If it actually reaches the edge then all the extractive profiles meet the rectifying profile.

The extractive profile approaches SN if there are enough stages in the extractive section. Thus, practically constant distillate purity can be maintained while component A is gradually boiled out from the still. Consequently, the process is feasible at a given reflux ratio if the feed ratio is greater than some minimum. This minimum can be determined by computing and visualizing the extractive profiles *from a single still composition* with increasing F/V, as illustrated in Figure 2, because all the extractive profiles approach the same stable node at a given F/V.

Feasibility of the BED process is more complicated at finite reflux ratios. First, there is a reflux ratio below which the rectifying profile is too short, shown in Figure 3. There is a sudden change in the length of the rectifying profile at some reflux ratio. Second, saddle point S_2 from the BE edge moves in the interior of the triangle and four separatrices are formed, as shown in Figure 4.

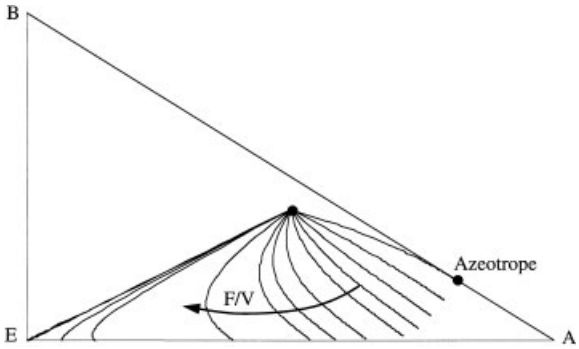

Figure 2. Path of the stable node SN can be determined by computing extractive profiles started from the same single point.

The pair of separatrices connecting the BE edge with SN through S_2 do not involve any obstacle against feasibility, but the other pair form a feasibility border because the extractive profiles to their left do not move toward SN. The still composition cannot be shifted across this border if the specified distillate composition is to be maintained. Thus, this pair of separatrices constitute a constraint to the still composition and, therefore, a constraint against total recovery of component A.

Interval Methodology

Interval methodology is a tool used to reliably find either all the solutions of a system of equations or all the global minimizers of a multivariate real function over a given domain. Robust interval methods are reliable in the sense they find all solutions in the studied region. If no solution is found in a domain then no solution exists there. If a solution cannot be excluded from a domain then its existence is either proven or probable. The latter case occurs if the local minimum of a real function is such a small positive value that can be considered approximately zero, and then its minimizer can be considered as a zero of this function. In some *degenerate cases*, there is an exact zero but it cannot be proven numerically. For example, $f(x) = (x - 1/3)^4$ has an exact zero value at 1/3, although 1/3 is not a member of the finite set of machine numbers. Because $f(x)$ does not have negative value, the existence of a zero cannot be proven, nor is it excluded, however.

Conventional search for zeros of a real function $f(x)$, that is, solutions of the equation $f(x) = 0$, leads to a sequence of real numbers $x^{(0)}, x^{(1)}, \ldots, x^{(k)}$, each of which is considered as an approximation of the root x^*. Such a sequence is either convergent or not, depending on the properties of the function and on the initial value $x^{(0)}$. If the sequence is convergent, it has a

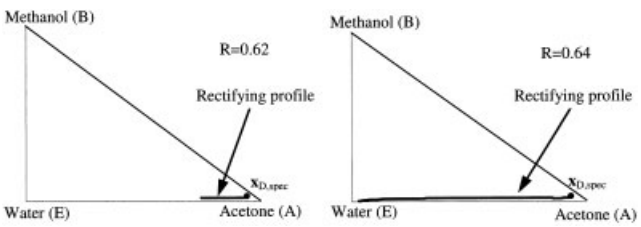

Figure 3. Sudden change in the length of the rectifying profile.

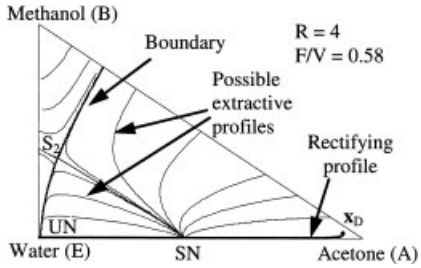

Figure 4. Profiles map at finite reflux ratio (feed ratio is above minimum).

limit point x^*. Even if it is convergent, it may alternatively converge to several different limit points $x^{*(1)}, x^{*(2)}, \cdots$, depending on the initial value $x^{(0)}$, if several zeroes exist. Moreover, it may happen that the sequence converges to a limit cycle of points $x^{*(1)}, x^{*(2)}, \ldots, x^{*(n)}$; that is, it may be attracted by a finite set of points in a way that these points are visited in a fixed order in an infinite loop. Dependency of the convergence on the initial value and on some parameters of $f(x)$ may show up fractal properties, as is pointed out by Feigenbaum[6] and subsequently by others (see, for example, Lucia et al.[7]).

Other methods applicable to find zeroes and global minima with mathematical exactness are available in the literature (see, for example, the αBB method of Maranas and Floudas[8] or the terrain method of Lucia and Feng[9]). These can be considered as "reliable" because they are exact in a mathematical sense. These methods are computationally more effective, that is, faster than interval methodologies. On the other hand, these methods do not consider the finite set of numbers used in digital computers.

Interval methodology is applied in the present article to reliably find all the points in question considering both mathematical exactness and the finite set of machine numbers.

Interval algebra does not compute or approximate the point values of real functions but approximates from *outside* the range of the real function over an interval. Multivariate intervals are rectangular sets, called *boxes*. The value of a so-called *interval extension* $F(X)$ of a *real function* $f(x)$ over an interval or box is also an *interval*. Point values are then parenthesized in as narrow intervals as possible. In practice, interval methods try to compute the lowest upper bound and the highest lower bound of the function over a given box. Such a computation is not always possible; good bounds are looked for, instead. In any event, the value of an interval function should be an outer bounding of the range of f over X:

$$f(x) \in F(X) \qquad \text{if } x \in X \tag{4}$$

Equation 4 is called "inclusion " property. Any well-defined real function can be extended in such a way that its interval version is defined over some interval domain, and the resulting interval is an outer bounding of the range of f over X. If the inclusion property holds, $F(X)$ is called an *inclusion function*.

The scenario is complicated with the technical difficulty that the set of real numbers are approximately represented by a finite subset of machine numbers. Care should be exercised to compute rounding always to outwards (outward rounding); that is, round up for the upper bound and round down for the lower

bound, so as not to lose a solution by excluding it from the studied interval just because of improper rounding.

The usual operations of addition, subtraction, multiplication, and division are well defined on interval sets. Division with an interval that contains zero can also be defined as one resulting in two (a positive and a negative) semi-infinite intervals. Elementary functions can be defined over intervals, as well. Some interval methods need the knowledge of the interval versions of the derivatives of the studied function. To achieve the enclosures of the derivatives of f in an easy and automatic way, *automatic differentiation* techniques are often built into interval arithmetic routines. Automatic differentiation (see, for example, Rall[10]) is an algorithmic tool that produces the derivative values parallel to the computation of the original function. Thus, analytical differentiation before the computations is not needed, nor is the numerical differentiation based on finite differences.

The central difficulty raised by the interval inclusion functions is that the resulting enclosures usually overestimate the range. The overestimation is caused by the fact that in most cases intervals corresponding to the same real variable occur more than once in an arithmetic expression, which is called the *dependency problem*. The most common basic principles applicable to obtain better enclosures for a given function are the reformulation of the arithmetic expression to decrease variable dependency and the application of more advanced interval inclusion functions (such as those using higher-order derivatives) instead of the natural interval extension.

Interval algebra has been developed in the last decades to such a stage that it can successfully be applied to reliably solve such small-scale problems as root finding, minimization, and integration. Middle-scale problems have also been solved in some particular cases. Multiple solutions are found by systematically partitioning the studied interval and then evaluating the subintervals.

Modern development of interval methodologies goes back to Moore.[11] Several good introductions to such topics as interval algebra, interval root search, and interval minimization are already available. See, for example, Alefeld and Herzberger,[12] Neumaier,[13] Hansen,[14] Hammer et al.,[15] or Albrecht et al.[16] Interval software tools have also been developed.[17]

The idea of applying interval methodology to determine global optima and roots has already found its way to the community of chemical engineering, as well. Stadtherr and co-investigators[18-26] have published an extensive literature on chemical engineering applications.

Interval arithmetic is a convenient tool to be applied in branch-and-bound (B&B) optimization algorithms, given that the lower and upper bounds of the objective and constraint function values over a box are calculated in an easy and reliable way. A prototype interval B&B algorithm for finding all solutions of the bound constrained global minimization problem

$$\min_{x \in X_0} f(x)$$

is as follows:

- *Step 1*: Let **L** be an empty list, let $A := X_0$ be the current box to be investigated, and set the iteration counter to $k := 1$. Set the upper bound of the global minimum f^u to be the upper bound of $F(X_0)$.
- *Step 2*: Subdivide A into s subboxes $A_1, \ldots, A_s$. Evaluate the inclusion function $F(A_i)$ for all the new subintervals and update the upper bound of the global minimum f^u as the minimum of the old value and the smallest upper bound of the objective function values $F(A_i)$, $i = 1, \ldots, s$.
- *Step 3*: Delete those parts of the new subintervals that cannot contain a global minimizer ("accelerating tools").
- *Step 4*: If the remaining subintervals satisfy the stopping criterion, then add them to the list **S** holding the enclosures of candidate solutions; otherwise, add them to the list **L**.
- *Step 5*: If **L** is empty, then return; **S** contains the enclosures of all global minimizers, and the enclosure of the global minimum is $[f^l, f^u]$, where f^l is the smallest lower bound of the function values among the elements of **S**.
- *Step 6*: Set A to be that of the subinterval from the list **L** that has the smallest lower bound on F, and remove this subinterval from the list.
- *Step 7*: Let $k := k + 1$ and go to Step 2.

To solve our problems, we decided to use a ready-made and available interval optimization tool, recently developed at the University of Szeged. The algorithm itself is an improved version of the global optimization procedure of the C-XSC Toolbox[15] and it is implemented using the PROFIL/BIAS interval arithmetic library of Knüppel.[27] The interval inclusion functions are evaluated with a combination of the natural interval extension and a first-order centered (mean-value) form.[28] The accelerating methods (Step 3 of the prototype algorithm) are the so-called monotonicity, midpoint, cutoff, and concavity tests, and a step of the interval-Newton–Gauss–Seidel iteration, all discussed in Hammer et al.[15] The interval subdivision rule is that designated "C/3" in Markót et al.[29] The stopping criterion of Step 4 is based on the width of the particular box: if all its components have a width smaller than a prescribed value ranging from 10^{-2} to 10^{-12}, depending on the particular application, then the box is inserted to **S**.

Beside the basic B&B procedure, the algorithm contains a verification procedure[30] based on the interval-Newton step to confirm the existence and local uniqueness of the candidate optimizers. Further details of the algorithm can be found in articles by Markót et al.[29] and Csallner et al.[31]

Note, that the above global optimization algorithm can be applied to solve both minimization problems and root finding problems, given that any root-finding problem

$$f_i(x_1, x_2, \ldots, x_N) = 0 \qquad i = 1, 2, \ldots, N \tag{5}$$

can be reformulated as an optimization problem

$$\min_{\mathbf{x}} \sum_{i=1}^{N} f_i^2(\mathbf{x}) \tag{6}$$

If Eq. 5 has a solution then it is a (global) minimizer of Eq. 6 because the sum of squares cannot be negative. That is, if the global minimum of Eq. 6 is guaranteed to be positive over a given search domain then Eq. 5 has no solution in that domain. Throughout our study, we apply this reformulation to determine zeroes of equations.

The numerical computations were run on a Pentium IV PC

Table 1. Antoine Parameters A_i, B_i, and C_i

I	A_i	B_i	C_i
A	7.11714	1210.595	229.664
B	8.08097	1582.271	239.726
E	8.07131	1730.63	233.426

(with 1 GB of RAM and a 1.4 GHz CPU) under a Linux operating system.

Thermodynamic Model and Data of an Example Problem

We consider separating acetone (component A) from methanol (component B), a mixture forming minimum boiling azeotrope at an x_{acetone} value of about 0.821, with the use of water (component E) as entrainer.

The vapor–liquid phase equilibrium is modeled with a modified Raoult–Dalton equation in the form of

$$y_i^* P = \gamma_i x_i p_i^\circ \qquad i \in \{\text{A, B, E}\} \tag{7}$$

where pure component vapor pressure p_i° is computed with the three-parameter Antoine equation:

$$\log p_i^\circ = A_i - \frac{B_i}{T - 273.14 + C_i} \qquad i \in \{\text{A, B, E}\} \tag{8}$$

and the activity coefficients γ_i are computed with the three-parameter NRTL (nonrandom, two-liquid) model in the form of

$$\ln \gamma_i = \frac{\sum_{j\in\{\text{A,B,E}\}} \tau_{ji} G_{ji} x_j}{\sum_{l\in\{\text{A,B,E}\}} G_{li} x_l} + \sum_{j\in\{\text{A,B,E}\}} \frac{x_j G_{ij}}{\sum_{l\in\{\text{A,B,E}\}} G_{lj} x_j} \times \left(\tau_{ij} - \frac{\sum_{n\in\{\text{A,B,E}\}} x_n \tau_{nj} G_{nj}}{\sum_{l\in\{\text{A,B,E}\}} G_{lj} x_j} \right) \qquad i \in \{\text{A, B, E}\} \tag{9}$$

$$\tau_{ij} = \frac{U_{ij}}{R_G T} \qquad i, j \in \{\text{A, B, E}\} \tag{10}$$

$$G_{ij} = \exp(-\alpha_{ij}\tau_{ij}) \qquad i, j \in \{\text{A, B, E}\} \tag{11}$$

Here U_{ij} represents the binary interaction parameters (energy differences) and $\alpha_{ij} = \alpha_{ji}$ represents the binary nonrandomness parameters. For mathematical completeness, the well-known model above is supplemented with the requirement of summing up the mole fractions to unity:

$$\sum_{i\in\{\text{A,B,E}\}} x_i = 1 \tag{12}$$

$$\sum_{i\in\{\text{A,B,E}\}} y_i^* = 1 \tag{13}$$

The model parameters are collected in Tables 1 and 2.

Throughout our study, the specified distillate composition is $\mathbf{x}_D$ = [0.94, 0.025, 0.035] (acetone, methanol, water). Pure water is applied in the entrainer feed, that is, $\mathbf{x}_F$ = [0.0, 0.0, 1.0].

Thus, the rectifying profile and the extractive profiles are modeled with differential equations with algebraic constraints, that is, differential–algebraic equations (DAEs). These are the system

Equations 1, 2, and 7–13 (RP)

for the rectifying profile, and the system

Equations 1, 3, and 7–13 (EP)

for the extractive profiles.

The profiles and their pinch points can be computed even outside of the composition triangle, but this opportunity is constrained to a small neighborhood around the triangle because of the mathematical form of the model Eqs. 7–13. Thus, we searched for pinch points up to $x_{\text{methanol}} \geq -0.1$, but no farther.

Singular Points

We are interested in determining the reflux ratio at which the length of the rectifying profile suddenly jumps. Here the number of pinch points changes from one to three, through a single point where this number is just two. Thus, we want to find all the singular (pinch) points of the rectifying profile at given R.

We are also interested in finding $(F/V)_{\min}$ at finite R. To achieve this aim, we have to determine the loci of the singular points of the extractive profiles, the number of singular point, and the feed ratio at which the number of such points in the triangle decreases from four to two. The location of S_2 is also important for guessing maximal recovery.

Singular points of (RP) and (EP) are characterized by a zero value of the differentials in Eq. 1. This is fulfilled when the right-hand side equals zero, that is, when

$$\mathbf{y}(\mathbf{x}) - \mathbf{y}^*(\mathbf{x}) = \mathbf{0} \tag{14}$$

Thus, singular points of (RP) satisfy the following algebraic equation system:

Equations 2 and 7–14 (SRP)

Singular points of (EP) satisfy the following algebraic equation system:

Equations 3 and 7–14 (SEP)

Equation systems (SRP) and (SEP) are reformulated in the same way as Eq. 5 is reformulated to an optimization problem

Table 2. NRTL Parameters U_{ij} and α_{ij}

i	j	U_{ij}	U_{ji}	$\alpha_{ij} = \alpha_{ji}$
A	B	399.395	−16.784	0.292
A	E	−47.613	1919.523	0.291
B	E	−347.817	−347.817	0.302

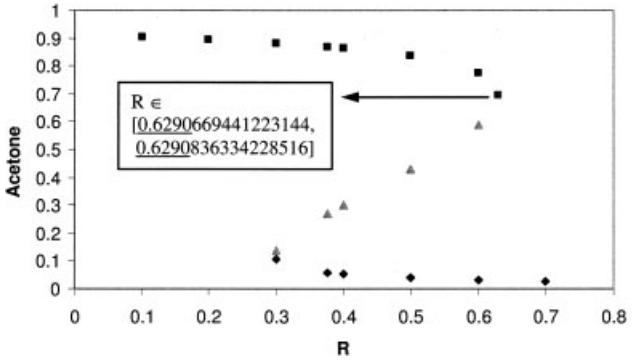

Figure 5. Plot of $x_{acetone}$ component of the found singular points in function of *R*.

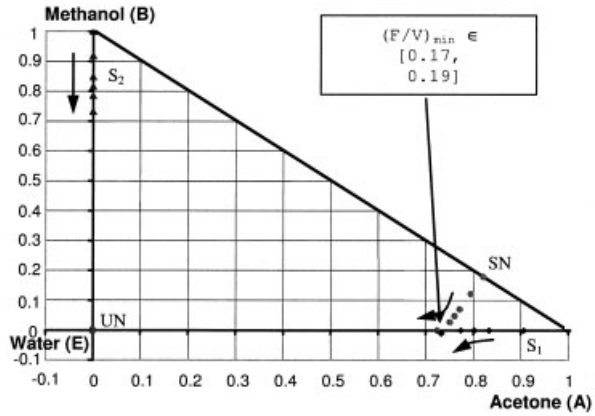

Figure 6. Singular point paths with evolving *F/V* at total reflux.

(Eq. 6). Values of U_{ij}, $\alpha_{ij} = \alpha_{ji}$, A_i, B_i, C_i $(i, j \in \{A, B, E\})$, R_G, P, and R are given; values of γ_i, p_i°, τ_i, G_{ij}, x_i, y_i, y_i^* $(i, j \in \{A, B, E\})$, x_E, and T are unknown in the case of SRP. The feed ratio F/V is an additional given value in the case of SEP. The equation systems are transformed to global minimization problems. The independent variables are x_A, x_B, and T. The searched box is {[0, 1], [0, 1], [200, 500]}. (Temperature is measured in degrees Kelvin.) The dependent variables are expressed and substituted. The objective function is

$$\sum_{i\in\{A,B,E\}} (y_i - y_i^*)^2$$

The whole range is not searched in one step. Instead, the composition triangle is preliminary subdivided to seven smaller subranges. The search is facilitated in this way. In some cases, this range is extended to include physically meaningless concentrations outside the triangle because the structure of the phase map can be better understood using information on the existence of singular points around the triangle. For this purpose, the lower bound 0 of a mole fraction is changed to -0.1. The range of at most a single variable is extended this way at each time.

Singular points of the rectifying profile (SRP)

Pinch points of the rectifying (enriching) profiles described by (RP), that is, solutions of (SRP), are found relatively easily by the solver.

The interval arithmetic tool is able to find all the pinch points at any specified R. As a result, a bifurcation diagram is plotted and shown in Figure 5. Stable points are denoted by squares lined up along imagined curves of a negative slope. Unstable nodes are denoted by triangles lined up along an imagined curve of a positive slope.

This bifurcation diagram explains the sudden change in the length of the rectifying profile. As the profile starts at a high x_A value, and evolves with decreasing x_A, the profile stops in the higher stable branch if R is <0.629. At higher reflux ratio, the profiles stop in the lower stable branch.

The rightmost standing square at about $R \approx 0.629$ and $x_{acetone} \approx 0.7$ is *not* found by this method. The nearer R is specified to this value, the longer time is consumed by the solver. In fact, no solution was reached in a week's time. This phenomenon must be caused by the fact that a bifurcation appears here.

Singular points of the extractive profiles map (SEP)

Pinch points of the extractive profiles described by equation system (EP), that is, solutions of (SEP), are also found relatively easily by the solver.

Four singular points of the extractive map are located in the arbitrary small neighborhoods of the three vertices and the azeotrope if total reflux is applied and F/V approaches zero. How these points are shifted with increasing F/V is shown in Figure 6. These points are determined using the interval arithmetic optimization tool with stepwise-incremented F/V. The stable node originating from the azeotrope moves along the isovolatility curve and meets another point moving from the acetone vertex along the acetone/water edge. The F/V value at which this meeting happens is $(F/V)_{min}$. At higher values the stable point moves on the same edge toward the water vertex. As a result, all the extractive profiles arrive at this point and cross the rectifying profile, with the consequence of feasibility.

All the singular points move in the interior of the triangle at decreasing R. Singular point paths are show in Figure 7 with $R = 4$. Unstable node UN originating from the water vertex is shifted so little that it practically remains stationary. Stable node SN does not move along the isovolatility curve but seems to emanate from a point on the acetone/methanol edge, close to

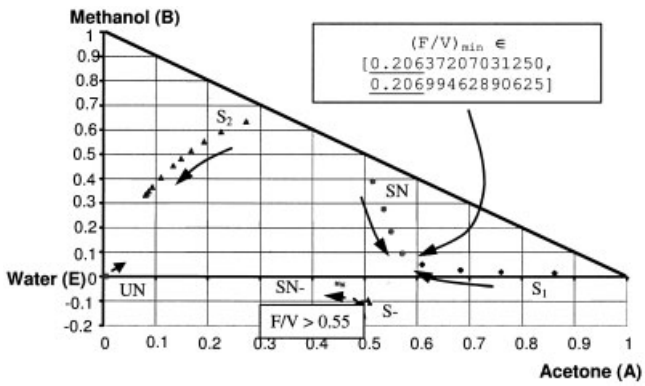

Figure 7. Singular point paths with evolving *F/V* at $R = 4$.

the azeotrope point. Saddle S_1, originating from the acetone vertex, does not move on the baseline. SN and S_1 meet inside the triangle at some particular F/V depending on R. As F/V is increased further, both SN and S_1 disappear.

Such a bifurcation occurs at $F/V \approx 0.207$; this is $(F/V)_{\min}$ if $R = 4$ is specified (Figure 7). Above this value the extractive profiles are directed toward a point somewhere outside the triangle. A second bifurcation occurs at $F/V \approx 0.55$. A new stable point SN- appears outside the physically meaningful composition triangle and moves toward the water vertex. There is also another saddle, S-, as its counterpart.

The most striking result is that the stable node originating from the azeotrope does not reach the acetone/water edge. Whereas the minimum feed ratio at total reflux ($R = \infty$) can be determined by tracing the location of SN in function of F/V to the A/E edge, this method cannot be applied in the case of finite reflux ratio because SN never touches the baseline. Instead, such an F/V is looked for at which SN and S_2 meet to disappear because above this value the attractive point is outside the triangle.

All the mentioned singular points are determined with stepwise-incremented F/V. The bifurcation points cannot be exactly determined in this way. The nearer the F/V is specified to this value, the longer the time is consumed by the solver.

Search for Bifurcation Points with Interval Methodology

Bifurcation points cannot be well approximated by simply determining the singular points with stepwise-incremented parameters because computation time increases to infinity as the bifurcation point is approximated. Instead, the criterion of bifurcation is applied as a new constraint in the model.

The character of a singular point can be analyzed by linearizing the differential equation in its neighborhood. Accordingly, Eq. 1 is approximated by

$$\frac{d\mathbf{x}}{dh} = \mathbf{A}\mathbf{x} \tag{15}$$

where matrix $\mathbf{A}$ is the Jacobian computed at the *singular* point $\mathbf{x}$.

Bifurcation points are characterized with zero real part of at least one eigenvalue of the Jacobian.[32-35]

All the singular points are characterized with only real eigenvalues in our case because the temperature changes monotonously along the solution of the autonomous differential equation. No focus may appear in the map. Consequently, irregularity is simply indicated by a zero determinant of $\mathbf{A}$. In this case, the criterion of bifurcation is

$$\det(\mathbf{A}) = 0 \tag{16}$$

The entries of the Jacobian $\mathbf{A}$ cannot be simply computed because the right-hand side of Eq. 1 depends on T, which, in turn, depends implicitly on x_A and x_B. The equilibrium temperature T cannot be algebraically discarded. In practice, we have the following relations:

$$a_{AA} = \frac{\partial}{\partial x_A} f_A(x_A, x_B, T)\bigg|_{x_A, x_B} \qquad a_{AB} = \frac{\partial}{\partial x_B} f_A(x_A, x_B, T)\bigg|_{x_A, x_B}$$
$$a_{BA} = \frac{\partial}{\partial x_A} f_B(x_A, x_B, T)\bigg|_{x_A, x_B} \qquad a_{BB} = \frac{\partial}{\partial x_B} f_B(x_A, x_B, T)\bigg|_{x_A, x_B} \tag{17}$$

where T is an implicit function ϑ of x_A and x_B:

$$T = \vartheta(x_A, x_B) \tag{18}$$

To determine the partial derivatives, the chain rule can be applied:

$$a_{ij} = \frac{\partial f_i(\mathbf{x}, T)}{\partial x_j}\bigg|_{\mathbf{x}, T=\vartheta(\mathbf{x})} + \frac{\partial f_i(\mathbf{x}, T)}{\partial T}\bigg|_{\mathbf{x}, T=\vartheta(\mathbf{x})} \times \frac{\partial \vartheta(\mathbf{x})}{\partial x_j}\bigg|_{\mathbf{x}} \qquad i \in \{A, B\}, j \in \{A, B\} \tag{19}$$

The partial derivatives of f_i according to the mole fractions can be expressed analytically, but the partial derivatives of ϑ according to the mole fractions are difficult to determine because function ϑ is not known explicitly. However, the implicit function theorem can be applied.

The bubble temperature T is determined according to the criterion of equilibrium expressed as Eqs. 7 and 13. A combination of these two equations leads to the criterion

$$P(x_A, x_B, T) = \gamma_E(x_A, x_B, x_E, T) x_E p_i^\circ(T) + \sum_{i \in \{A,B\}} \gamma_i(x_A, x_B, x_E, T) x_i p_i^\circ(T)$$
$$x_E = 1 - x_A - x_B \tag{20}$$

The differential of P according to mole fraction x_A or x_B should be zero because P is specified as a constant:

$$\gamma_k p_k^\circ - \gamma_E p_E^\circ + \sum_{i \in \{A,B\}} x_i \left[p_i^\circ \left(\frac{\partial \gamma_i}{\partial T} - \frac{\partial \gamma_E}{\partial T} + \frac{\partial \gamma_i}{\partial x_k} - \frac{\partial \gamma_E}{\partial x_k} \right) + \gamma_i \frac{dp_i^\circ}{dT} \right] = 0 \qquad k \in \{A, B\} \tag{21}$$

From here, the derivatives of T can be determined as

$$\frac{\partial \vartheta}{\partial x_j}\bigg|_{\mathbf{x}} = -\frac{\dfrac{\partial(x_A, x_B, T)}{\partial x_j}}{\dfrac{\partial(x_A, x_B, T)}{\partial T}} \tag{22}$$

Thus, the bifurcation points of (RP) can be located by finding the roots of the equation system

Equations 2, 7–12, 14, 16, and 19 (BRP)

and the bifurcation points of (EP) can be located by finding the roots of the equation system

Equations 3, 7–12, 14, 16, and 19 (BEP)

There are several ways to numerically locate bifurcation points. Applications are available in the chemical engineering literature.[36-39] Interval methodology is also applied (see, for example, Tolsma and Barton,[40] Gehrke and Marquardt,[41] or Gwaltney et al.[42]).

In the present article, however, simple singular points and bifurcations are determined with the same tool. Equation systems (BRP) and (BEP) are reformulated in the same way as equation systems (SRP) and (SEP) are, but the objective function as appended with the square of the determinant

$$\sum_{i\in\{A,B,E\}} (y_i - y_i^*)^2 + [\det(\mathbf{A})]^2$$

The results are collected in Tables 3 and 4. The numbers shown in these tables are lower and upper bounds to the exact values according to the applied model. All the displayed digits are valid as a result of the outward rounding methodology. The upper bounds are shown below the lower bounds; the identical leading digits are underlined for easy comparison. The same convention is applied in Figures 6 and 7. Although so many digits seem meaningless in practice, one can be sure that the solution is somewhere between the two bounds.

Conclusions

An interval arithmetic–based branch-and-bound optimization tool is applied to analyze the feasibility of batch extractive distillation. Using this tool, we are able to reliably find all the singular points of the profile maps. This tool is also successfully applied to find bifurcation points.

Upon examining the extractive profiles map of the acetone (A)–methanol (B)–water (E) system, we find that there are four singular points (two saddles, a stable node, and an unstable node) at higher reflux ratios. At total reflux and increasing feed ratio, the two saddles move along the AE and the BE edges, respectively, toward the water vertex (component E); the stable node meets the saddle on the AE edge and they change stability. At finite reflux ratio, the singular points are found inside the triangle; the stable node and the saddle point initiating from vertex A collide and bifurcation occurs. Both colliding singular points vanish after the collision and the profiles lead out from the triangle through the AE edge. The minimum feed ratio can be determined by computing the bifurcation point. The reflux ratio at which the rectifying profile suddenly changes its length can be found in the same way.

Table 3. Bifurcation Point Interval of the Specified Rectifying Profile

R	0.6290669441223144
	0.6290836334228516
x_{acetone}	0.6932788372039798
	0.6932974338531500
x_{methanol}	0.0201442718505859
	0.0201454162597657
T (K)	333.1959158182144165
	333.1962019205093384

Table 4. Bifurcation Point Intervals of the Extractive Profiles Map at Two Reflux Ratios

	$R = 4$	$R = 10$
F/V	0.2063720703125000	0.1578170891437115
	0.2069946289062501	0.1585855111005144
x_{acetone}	0.5877075195312502	0.7042266845703127
	0.5881469726562504	0.7047851562500003
x_{methanol}	0.0673706054687500	0.0400826140894999
	0.0677490234375001	0.0404432357242396
T (K)	333.9262008666992187	332.6806640624999999
	333.9355468750000001	332.6953125000000001

Acknowledgments

This research was partially supported by Hungarian National Research Fund (OTKA) grants F 046282, T 048377, T 046822, T 037191, and T 062099.

Notation

a = element of the Jacobian matrix
A, B, C = Antoine coefficients in Eq. 8
A, B, E = components
D = distillate flow rate
$f(\mathbf{x}, T)$ = righthand side of Eq. 1, taking into account the explicitly unknown boiling point
$f(x)$ = real function
$F(X)$ = interval extension of $f(x)$
F = entrainer flow rate
F/V = feed ratio
G, U = parameters in the NRTL equation
h = dimensionless height
L = liquid flow rate
N = number of components (in the NRTL equation)
P = total pressure
p° = vapor pressure of a pure component
R = reflux ratio
S = saddle
SN = stable node
T = temperature
UN = unstable node
V = vapor flow rate
X = interval
x, $\mathbf{x}$ = mole fraction in liquid phase
$y(\mathbf{x})$ = actual mole fraction in gas phase (operating line)
$y^*(\mathbf{x})$ = equilibrium mole fraction in gas phase

Greek letters

γ = activity coefficient
$\vartheta(\mathbf{x})$ = bubble point function of the mole fractions
τ, α = parameters in the NRTL equation

Subscripts and superscripts

$*$ = vapor–liquid equilibrium
$^\circ$ = pure component
A, B, E = components A, B, E
D = distillate
F = feed
i, j = components i, j
min = minimal (ratio)
S = still
SN = stable node

Literature Cited

1. Stéger C, Varga V, Horváth L, Rév E, Fonyó Z, Meyer M, Lelkes Z. Feasibility of extractive distillation process variants in batch rectifier column. *Chem Eng Proc.* 2005;44:1237-1256.
2. Lelkes Z, Lang P, Benadda B, Moszkowicz P. Feasibility of extractive distillation in a batch rectifier. *AIChE J.* 1998;44:810-822.
3. Lelkes Z, Rév E, Stéger Cs, Fonyó Z. Batch extractive distillation of maximal azeotrope with middle boiling entrainer. *AIChE J.* 2002;48: 2524-2536.
4. Rév E, Lelkes Z, Varga V, Stéger Cs, Fonyó Z. Separation of minimum boiling binary azeotrope in batch extractive rectifier with intermediate boiling entrainer. *Ind Eng Chem Res.* 2003;42:162-174.
5. Safrit BT, Westerberg AW, Diwekar U, Wahnschafft OM. Extending continuous conventional and extractive distillation feasibility insights to batch distillation. *Ind Eng Chem Res.* 1995;34:3257-3246.
6. Feigenbaum MJ. Quantitative universality for a class of nonlinear transformations. *J Stat Phys.* 1978;19:25-52.
7. Lucia A, Guo XZ, Richey PJ, Derebail R. Simple process equations, fixed-point methods, and chaos. *AIChE J.* 1990;36:641-654.
8. Maranas CD, Floudas CF. Finding all solutions of nonlinearly constrained systems of equations. *J Glob Opt.* 1995;7:143-182.
9. Lucia A, Feng Y. Multivariable terrain methods. *AIChE J.* 2003;49: 2553-2563.
10. Rall LB. *Automatic Differentiation: Techniques and Applications.* Berlin/New York: Springer-Verlag; 1981.
11. Moore RE. *Interval Analysis.* Englewood Cliffs, NJ: Prentice-Hall; 1966.
12. Alefeld G, Herzberger J. *An Introduction to Interval Computation.* New York: Academic Press; 1983.
13. Neumaier A. *Interval Methods for Systems of Equations.* Cambridge, UK: Cambridge Univ. Press; 1990.
14. Hansen E. *Global Optimisation Using Interval Analysis.* New York: Marcel Dekker; 1992.
15. Hammer R, Hocks M, Kulisch U, Ratz D. *Numerical Toolbox for Verified Computing I.* Berlin: Springer-Verlag; 1993.
16. Albrecht R, Alefeld G, Stetter HJ, eds. *Validation Numerics—Theory and Applications.* Vienna/New York: Springer-Verlag; 1993.
17. University of Texas at El Paso. *Interval and Related Software*. Available at http://www.cs.utep.edu/interval-comp/intsoft.html (Accessed at April 25, 2006).
18. Hua JZ, Brennecke JF, Stadtherr MA. Reliable phase stability analysis for cubic equation of state models. *Comp Chem Eng.* 1996;20:S395-S400.
19. Hua JZ, Brennecke JF, Stadtherr MA. Enhanced interval analysis for phase stability: Cubic equation of state models. *Ind Eng Chem Res.* 1998;37:1519-1527.
20. Maier RW, Brennecke JF, Stadtherr MA. Reliable computation of homogeneous azeotropes. *AIChE J.* 1998;44:1745-1755.
21. Maier RW, Brennecke JF, Stadtherr MA. Reliable computation of reactive azeotropes. *Comp Chem Eng.* 2000;24:1851-1858.
22. Tessier SR, Brennecke JF, Stadtherr MA. Reliable phase stability analysis for excess Gibbs energy models. *Chem Eng Sci.* 2000;55: 1785-1796.
23. Stradi BA, Brenecke JF, Kohn JP, Stadtherr MA. Reliable computation of mixture critical points. *AIChE J.* 2001;47:212-221.
24. Gau CY, Stadtherr MA. New interval methodologies for reliable chemical process modeling. *Comp Chem Eng.* 2002;26:827-840.
25. Scurto AM, Xu G, Brennecke JF, Stadtherr MA. Phase behavior and reliable computation of high pressure solid–fluid equilibrium with cosolvents. *Ind Eng Chem Res.* 2003;42:6464-6475.
26. Lin Y, Stadtherr MA. LP strategy for interval-Newton method in deterministic global optimization. *Ind Eng Chem Res.* 2004;43:3741-3749.
27. Knüppel O. *PROFIL—Programmer's Runtime Optimized Fast Interval Library.* Hamburg, Germany: Technische Universität Hamburg; 1993.
28. Ratschek H, Rokne J. *Computer Methods for the Range of Functions.* Chichester, UK: Ellis Horwood; 1984.
29. Markót MC, Csendes T, Csallner AE. Multisection in interval branch-and-bound methods for global optimization. II. Numerical tests. *J Glob Opt.* 2000;16:219-228.
30. Csendes T, Ratz D. Subdivision direction selection in interval methods for global optimization. *SIAM J Numer Anal.* 1997;34:922-938.
31. Csallner AE, Csendes T, Markót MC. Multisection in interval branch-and-bound methods for global optimization. I. Theoretical results. *J Glob Opt.* 2000;16:371-392.
32. Kunzentsov YA. *Elements of Applied Bifurcation Theory.* 2nd Edition. New York: Springer-Verlag; 1998.
33. Guckenheimer J, Holmes P. *Nonlinear Oscillations, Dynamical Systems and Bifurcations of Vector Fields.* New York: Springer-Verlag; 1983.
34. Golubitsky M, Schaeffer DG. *Singularities and Groups in Bifurcation Theory*. Vol. I. New York: Springer-Verlag; 1985.
35. Seydel R. *Practical Bifurcation and Stability Analysis: From Equilibrium to Chaos.* New York: Springer-Verlag; 1994.
36. Knapp JP, Doherty MF. Minimum entrainer flows for extractive distillation—A bifurcation theoretic approach. *AIChE J.* 1994;40:243-268.
37. Fidkowski ZT, Doherty MF, Malone MF. Feasibility of separation for distillation of nonideal ternary mixtures. *AIChE J.* 1993;39:1303-1321.
38. Krolikowski LJ. Determination of distillation regions for non-ideal ternary mixtures. *AIChE J.* 2006;52:532-544.
39. Dorn C, Morari M. Qualitative analysis for homogeneous azeotropic distillation. 2. Bifurcation analysis. *Ind Eng Chem Res.* 2002;41:3943-3962.
40. Tolsma JE, Barton PI. Computation of heteroazeotropes. Part II: Efficient calculation of changes in phase equilibrium structure. *Chem Eng Sci.* 2000;55:3835-3853.
41. Gehrke V, Marquardt W. A singularity theory approach to the study of reactive distillation. *Comp Chem Eng.* 1997;21:S1001-S1006.
42. Gwaltney CR, Styczynski MP, Stadtherr MA. Reliable computation of equilibrium states and bifurcations in food chain models. *Comp Chem Eng.* 2004;28:1981-1996.

Manuscript received Feb. 2, 2006, and revision received May 8. 2006.